One-dimensional evaporative cooling of magnetically trapped atomic hydrogen

P. W. H. Pinkse,* A. Mosk, M. Weidemüller,† M. W. Reynolds, and T. W. Hijmans
Van der Waals–Zeeman Instituut, Universiteit van Amsterdam, Valckenierstraat 65, 1018 XE Amsterdam, The Netherlands

J. T. M. Walraven
FOM Institute for Atomic and Molecular Physics (AMOLF), Kruislaan 407, 1098 SJ Amsterdam, The Netherlands

(Received 5 January 1998)

We report experiments on evaporative cooling of spin-polarized atomic hydrogen gas confined in a cryogenic magnetic trap, and present a model of the trapped gas based on a generalized truncated Boltzmann approximation for the phase-space distribution function. The model takes into account the dimension of the evaporation [three-dimensional (3D) or 1D] and the time dependence of both the depth and the shape of the confining potential. Our observations are consistent with 1D evaporative cooling. To attain maximal phase-space density, we used the model assuming 1D evaporative cooling to optimize the evaporation procedure. With this work, the low dimension of evaporation was identified as the bottleneck thus far preventing us from achieving Bose-Einstein condensation in trapped atomic hydrogen.
[S1050-2947(98)08006-8]

PACS number(s): 03.75.Fi, 67.65.+z, 32.80.Pj

I. INTRODUCTION

Since its introduction for magnetically trapped atomic hydrogen [1–3], evaporative cooling has proven to be a powerful technique to increase the phase-space density of trapped gases. It was used, in the case of alkali vapors, to reach the critical density required for Bose-Einstein condensation (BEC) [4]. As the only cooling technique currently applicable at high phase-space density, it plays a central role in the rapidly expanding field of BEC in ultracold gases [5].

Evaporative cooling occurs when energetic atoms are lost from a trap as a result of elastic interatomic collisions. These atoms carry with them a disproportionate share of the thermal energy, and the remaining trapped atoms collisionally equilibrate to a lower temperature. The availability of energetic atoms decreases exponentially as the ratio of trap depth to temperature increases, so to keep evaporation going it is necessary to decrease the trap depth to track the temperature (forced evaporation).

The most efficient form of evaporative cooling is plausibly ''ergodic'' evaporation, in which all atoms acquiring a total energy exceeding the depth of the trap are quickly lost. In this case the rate of evaporation is just the rate at which interatomic collisions promote atoms to energies higher than the trap depth. Experimentally, efficient evaporation can result when an equipotential surface of the trap is made absorbing, for example with material walls [6], a microwave resonance [7], or an optical resonance [8]. Then atoms with sufficient energy to reach the equipotential are efficiently pumped from the trap, and the evaporation is almost ergodic [9].

However, evaporation can be much less efficient than in the ideal situation. As discussed by Surkov, Walraven, and Shlyapnikov, whether the collisionless motion of the atoms in the magnetic trap is regular or stochastic can have profound consequences for the efficiency of evaporative cooling [10]. An important notion is the ''effective dimension of evaporation'' [10]. Ergodic evaporation is ''three dimensional'' (3D), since the criterion for the escape of an atom from the trap is based on the total energy of the atom. In the situation where the motional degrees of freedom of the atom are uncoupled and the energy of motion in only one direction determines the escape, the evaporation is ''one dimensional'' (1D). Everything else being the same, the rate of 1D evaporation is slower than that of 3D evaporation by a factor approximately four times the dimensionless ratio of the trap depth to the temperature of the gas [10].

In practice, to compete with other processes that lead to atom loss and heating, fast 3D cooling is to be preferred. It is hard to realize true three-dimensional evaporative cooling [5]. For example, for the heavier alkalis gravity will displace the surface of constant potential energy from the magnetic resonance (rf) ejection surface, which removes the energetic atoms and in this way will reduce the dimensionality of the evaporation (bottlenecking of the evaporation process). Despite its expected ubiquity, no investigation of 1D evaporation has yet been reported.

In this paper we present a detailed analysis of our evaporative cooling experiments, and present a model of the trapped gas based on a generalized truncated Boltzmann approximation for the phase-space distribution function. The model can be configured to describe 3D or 1D evaporative cooling, including the time dependence of both the depth and shape of the confining potential. Our observations are consistent with the 1D evaporative-cooling version of our model. To attain maximal phase-space density, we optimized the evaporation procedure, using the knowledge that the evaporation process is consistent with 1D evaporation.

The paper is organized around two main parts: the first part describes the experiments, and the second is devoted to a description of the 1D and 3D evaporation models. After a brief introduction of our assumptions and terminology in

*Present address: Fakultät für Physik, Universität Konstanz, Fach M701, D-78457 Konstanz, Germany.

†Present address: Max-Planck-Institut für Kernphysik, Saupfercheckweg 1, D-69117 Heidelberg, Germany.

Sec. II A, and trapping potentials in Sec. II B, we present the apparatus (Sec. III A) and the experiments showing the low dimensionality of the evaporation (Sec. III B). Following this, we present measurements of forced evaporative cooling experiments (Sec. III C) that were optimized to reach a high phase-space density. The second part of the paper starts with a general discussion of the evaporation model (Sec. IV), followed by the details for the 1D (Sec. V) and 3D cases (Sec. VI). Finally, we discuss the implications of the dimensionality of evaporation for the attainment of Bose-Einstein condensation of atomic hydrogen in our apparatus.

II. PRELIMINARIES

A. Physical picture

The description of evaporative cooling in this paper is based on the model introduced in Refs. [11] and [12]. We consider a nondegenerate Bose gas, confined by an external potential $U(\mathbf{r})$ in which the atoms move quasiclassically. The gas is described by the distribution of atoms in phase space (the space of atomic position $\mathbf{r}$ and momentum $\mathbf{p}$). The energy of an atom, ϵ, is given by $\epsilon = p^2/2m + U(\mathbf{r})$, where m is the atom mass. Interactions between the atoms provide collisions, but we neglect their contribution to the energy, as the density of atoms is low. We assume that the phase-space distribution is thermal, characterized by a temperature T, in the generalized sense of Ref. [12], even when the trap depth is finite and the gas is evaporating. This means that in the part of phase space occupied by trapped atoms the phase-space density is proportional to $\exp(-\epsilon/kT)$, with k the Boltzmann constant. The peak phase-space density (often called simply the ''phase-space density'') is written $n_0\Lambda^3$, where n_0 is a real-space atom density, called the ''reference density,'' and Λ is the thermal de Broglie wavelength, defined by $\Lambda = (2\pi\hbar^2/mkT)^{1/2}$. Typically n_0 is approximately equal to the actual real-space density at the center of the trap; this equality becomes exact in the limit of an infinitely deep trap. For a given trapping potential, the state of the gas is completely determined by the variables n_0 and T, which form a natural basis for a thermodynamic description of evaporative cooling. The number of atoms in the trap, N, is related to the reference density by the effective volume V_e, defined by $V_e = N/n_0$. The external potential can be usefully characterized by the exponent γ which describes how V_e scales with temperature: $V_e \propto T^\gamma$. From a perfectly isolated, infinitely deep trap, atoms can only escape by internal decay processes. In our experiments, spin-dipole relaxation [13] was the dominant loss mechanism. Dipolar relaxation leads to loss of particles and to heating. Because it is a two-body process, it becomes more important at high densities. In order to cool the gas to low temperatures and high densities, an efficient cooling process, such as evaporative cooling, is required.

The simplest way to model evaporative cooling is to consider a fixed potential with a variable cutting edge, that determines the depth of the trap, as was done in Refs. [11] and [12]. However, in many situations (including our experiments) it is impossible to lower only the trap depth without changing the rest of the trapping potential. The question addressed in this paper is that of what happens under a general potential change of a trap of finite depth? A quantitative answer will be given in later sections. Here we discuss this point qualitatively, in order to define the different processes and to clarify the terminology.

In our modeling we assume that states can be categorized as trapped or untrapped. *Evaporation* occurs when atoms are promoted to untrapped states by collisions with other atoms. Atoms in untrapped states are assumed to leave the trap before colliding with another atom (no collisional recapture). For this, the gas should be in the Knudsen regime—the mean free path of an atom should exceed the size of the gas cloud, which is a typical situation for most experiments. In contrast to the assumptions in Refs. [11] and [12], the condition that discriminates the trapped atoms from the untrapped atoms is not only a function of the total energy. The 3D and 1D evaporation processes differ in the criterion (the escape criterion) which distinguishes trapped states from untrapped states. For 3D evaporation the escape criterion involves simply the total energy of the atom. For 1D evaporation the energy associated with the motion of an atom in a particular direction (the escape direction) should be considered.

It is worth mentioning that the question of whether the evaporation is 3D or 1D can depend on the gas density, even when maintaining the condition of having a Knudsen gas. When the collision time is longer than the ergodic mixing time at low density (giving 3D evaporation), it may be shorter at high density (giving 1D evaporation if there is a single escape direction). To avoid dealing with this crossover between 3D and 1D evaporation, in this paper we only consider cases where the degrees of freedom of the collisionless motion of atoms are either completely mixed (full ergodicity), or not mixed at all.

Atoms that are lost because the trap becomes too shallow to confine them are said to be *spilled* [12]. In a quantum-mechanical picture these are the particles that occupy states that are removed from the trap. Spilling is a single-particle process that is independent of collisions. If spilling is done quickly (faster than the collision rate) it can be used to analyze the energy distribution of the trapped atoms [14]. In forced evaporative cooling the trap depth is lowered to increase the evaporation rate. It is important to bear in mind that the atoms spilled as a direct result of this lowering are not, properly speaking, evaporated, and they do not change the temperature directly. They are simply lost, leaving the rest of the distribution function unchanged.

A simple case of spilling occurs when only the trap depth is lowered in an otherwise unchanged potential. We refer to this case as ''pure spilling.'' Spilling in most alkali experiments is pure spilling, because the trap depth is lowered by reducing the frequency of the rf field, which can be realized independently from the magnetic trapping field. On the other hand, it is not necessary to decrease the trap depth to spill atoms. For instance, when adiabatically compressing a gas, e.g., by increasing the spring constant of a harmonic trap, but keeping the trap depth constant, the level splitting increases, and states are forced out of the trap.

Work is done by (or on) the trapped gas if the trapping potential is varied. We consider variations of the potential on a time scale sufficiently slow in comparison with the collision time that the thermal character of the distribution is not appreciably disturbed. In this case, for example, increasing the spring constants of a harmonic trap leads to adiabatic

compression and heating of the gas. If work is done sufficiently slowly, it is a reversible process that does not change the entropy of the gas. This also holds for slow adiabatic changes of the trapping potential that change γ, in which case the phase-space density can be changed in a reversible way [15].

B. Trapping potentials

In our experiments evaporation is 1D because the longitudinal and transverse degrees of freedom of atomic motion are uncoupled, and only the longitudinal motion of the atoms determines their escape from the trap. Our trap is of the Ioffe type [16], and its potential can be approximated by

$$U(x,y,z)=\sqrt{\alpha^2(x^2+y^2)+[U_0+U_z(z)]^2}-U_0, \quad (1)$$

where $U_z(z)$ is determined by the axial coils and can have a complicated shape, and $U_z(z_0)=0$, where z_0 is the coordinate of the trap minimum. The potential offset parameter U_0 is determined by the magnetic field at the trap minimum. The leading off-axis behavior is described by the transverse potential gradient α due to the Ioffe bars. An important special case is the trap we call Ioffe quadrupole (IQ), for which the axial potential U_z is harmonic, $U_z(z)=\beta z^2$. For an infinitely deep IQ trap the three parameters U_0, α, and β describe the potential completely.

In addition to the supposed infinitely extending magnetic trapping potential, usually a surface is present at which atoms are removed from the trap. We assume here that this surface coincides with an equipotential surface of truncation energy ϵ_t. Atoms with a trajectory crossing this surface are thought to be removed from the trap immediately. Note that if the potential energy is chosen to be zero at the trap minimum, as we will assume throughout this paper, ϵ_t is just the depth of the trap (in the direction of the pumping surface, at least).

As shown in Ref. [17], when $U_0>\epsilon_t$ the transverse and longitudinal degrees of freedom in a Ioffe trap are effectively uncoupled. This conclusion was reached considering the Ioffe potential, including small terms beyond the approximation of Eq. (1). It is noteworthy that for typical Ioffe traps the ratio of transverse and longitudinal oscillation frequencies is large, which makes this uncoupling a robust phenomenon. When working at ultralow temperatures the condition $U_0 \gg kT$ is inevitable in our Ioffe trap, and because ϵ_t is not so very much greater than kT, one can easily appreciate that uncoupling is essentially unavoidable in practice.

When U_0 is much larger than ϵ_t the potential is separable in its variables—to a very good approximation—and we may write the potential as

$$U(x,y,z)=U_\perp(x,y)+U_z(z), \quad (2)$$

the sum of the longitudinal potential $U_z(z)$ and a transverse potential which is essentially harmonic, $U_\perp(x,y)=m\omega_\perp^2(x^2+y^2)/2$. The oscillation frequency for the transverse motion is given by $\omega_\perp=\alpha/\sqrt{mU_0}$. If the potential is separable, the energy ϵ of an atom can be considered to be the sum of a transverse energy, $\epsilon_\perp$, and a longitudinal energy, ϵ_z, which are uncoupled (between collisions) and conserved (for a constant trap). In our 1D evaporation model we will discuss traps of the form of Eq. (2) with evaporation determined by the longitudinal potential U_z. We will give expressions for general U_z and harmonic $U_\perp$.

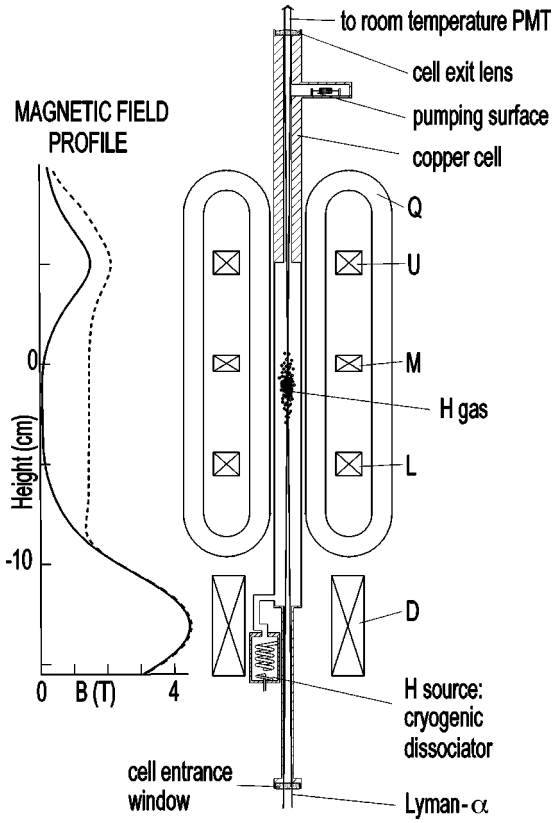

FIG. 1. Schematic of the apparatus. On the right side an overview of the experimental cell is sketched, together with the superconducting coils forming the magnetic trap. The axial confinement coils are labeled, from top to bottom, *U* (upper), *M* (middle), *L* (lower), and *D* (dissociator). The set of four racetrack coils creating the radial confining field are indicated with *Q*. Also shown is the Lyman-α beam path for optical spectroscopy of the trapped gas. On the left side a possible field profile, along the axis and along the wall, is indicated.

A general class of separable potentials was analyzed in Ref. [18]. These potentials are of the form

$$U(x,y,z)=(x/\lambda_x)^{1/\delta_x}+(y/\lambda_y)^{1/\delta_y}+(z/\lambda_z)^{1/\delta_z}, \quad (3)$$

where, e.g., λ_x sets the length scale in the x direction, and δ_x sets the power law. The harmonic trap is a special case, with $\delta_x=\delta_y=\delta_z=\frac{1}{2}$, and, e.g., $\lambda_x=\omega_x\sqrt{2/m}$. We will give expressions for this class of traps as well.

III. EXPERIMENTS

A. Apparatus

In our experiments we use the cryogenic Ioffe trap which was described in detail elsewhere [19]. It consists of four racetrack- (oval-) shaped coils providing radial confinement, and a set of four cylinder-symmetric axial confinement coils, creating magnetic-field profiles such as that shown in Fig. 1. The potential is approximately given by Eq. (1).

The trap is loaded with atomic hydrogen produced by dissociation of molecular hydrogen in a cryogenic discharge, and thermalized into the trap by collisions of the atoms with

the helium-coated wall and with each other. To obtain high densities, the superfluid ^{4}He film was covered with a monolayer of ^{3}He. A typical sample just after loading consists of 10^{12} atoms at a temperature of 70 mK. At the start of the experiment, the wall of the experimental cell can play a role, as in Ref. [6], but the sample quickly cools away from the wall, and the depth will be determined by a maximum of a magnetic field barrier as will be assumed in the rest of this paper. Evaporative cooling is performed by varying the currents in the axial coils to reduce the depth of the trap. Atoms escaping from the trap are cryopumped away.

It is important to note that our trap is constructed with superconducting coils optimized primarily to sustain a high trap depth with minimal dissipation (using persistent current switches), rather than fine control over the field. The uncertainties in the trap depth are estimated to be on the order of 0.5 mT. Careful attention had to be paid to current lag because of the high self-inductances of the coils and the finite resistance of the normal state of the persistent-current switches. Fortunately, most of these parameters are known, and the current lag in the coils can be anticipated when programming a field change by integrating the differential equations connecting the magnet power supply currents with the actual currents in the coils, taking into account the relaxation time due to the protection, and switch resistors which shunt the superconducting coils [20].

The trapped gas is probed optically, using narrow-band light resonant with the Lyman-α transition (wavelength $\lambda = 122$ nm). The light beam is passed through the gas (see Fig. 1), and the total transmission is measured as a function of frequency. Comparison with theoretical spectra enables us to characterize the trapped gas by, e.g., its temperature and peak density. Details of the spectroscopic technique can be found in Ref. [21].

B. Experimental evidence of 1D evaporation

The question of whether evaporation in our experimental situation is better described by 1D or 3D evaporation was answered by the experiment described in this section. An evaporation experiment was performed starting with samples of 1.7×10^{11} atoms at 25 mK with a density of 3×10^{12} cm^{-3}, as determined by Lyman-α spectroscopy. Next, the trap depth was reduced from 0.15 K to a value less than 0.1 mK (dashed line in Fig. 2), by lowering the upper confinement barrier. In this case this was done by reducing the current in the M coil in four linear sweeps. As a consequence the trap depth changes relatively fast at the end of the procedure. After the reduction of the trap depth, the sample was probed by taking Lyman-α spectra of 10-s duration, and found to have temperatures of about 1 mK.

We simulated the evolution of the gas using two versions of our evaporation model, one simulating 3D evaporation and the other simulating 1D evaporation. Both versions of the model will be described later in this paper in detail. For computational efficiency we assume that the trap is effectively harmonic in the z direction (IQ trap). The full expressions for the field are used to find the truncation energy ϵ_t and from the behavior of $U(\mathbf{r})$ near its minimum, the trap parameters α, β, and U_0. The real trap was then approximated by an IQ trap with these parameters. In the 1D case we found no significant difference when the full z dependence was replaced by the IQ approximation. We do not expect significant differences in the 3D case either.

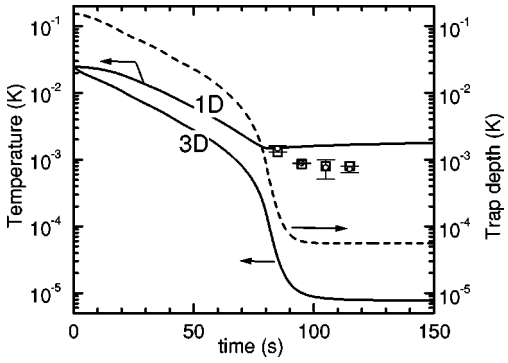

FIG. 2. Plot of the trap depth and the temperatures predicted by the 3D and 1D evaporation models vs time, during lowering of the current through one of the axial confinement coils. The symbols are measured data points. The initial condition is a density of 3×10^{12} cm^{-3} and a temperature of 25 mK. The conditions are chosen such as to accentuate the difference between 1D and 3D evaporation.

The results of the simulations are shown in Fig. 3, together with temperature and density obtained from the spectra. The evolution calculated for 3D evaporation predicts a monotonously increasing density and decreasing temperature, while the 1D evaporation gives rise to a sharp decline in density after an initial modest increase. Once the trap depth is lower than the ''temperature,'' cooling ceases (in the 1D case), because an evaporating particle carries away insufficient energy. In this case the momentum distribution of atoms in the trapped gas cloud is a disk in the (v_x,v_y) plane. One might well expect that the models, based on the truncated Boltzmann distribution, will become inaccurate when η (the ratio of trap depth to temperature) becomes of order unity. It is hence not surprising that the data are not in quantitative agreement with either model. The data are, however, consistent with the 1D evaporation model, and not at all with the 3D evaporation model. The 1D truncation of the phase-space distribution is taken into account when calculating theoretical Lyman-α spectra for the determination of tempera-

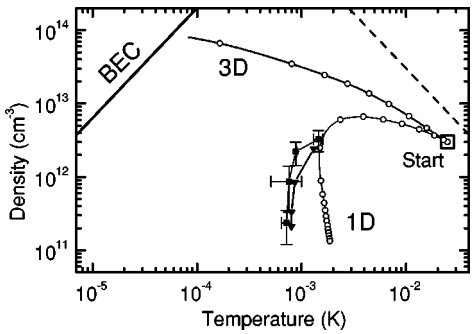

FIG. 3. The same results as in Fig. 2, now plotted in the T-n_0 plane, showing results of simulations employing 3D and 1D evaporation. The open circles are spaced 10 s apart. The dashed line indicates the slope for a trajectory without atom loss (assuming a harmonic potential). The solid symbols are experimental points, starting at $t=85$ s, spaced 10 s apart, in two series of measurements. The error bars on one of the series are obtained by fitting with different approximations to the Lyman-α beam profile.

ture and density from the data. Using a 3D-truncated distribution leads to even lower derived densities and makes the discrepancy between the 3D model and these data even larger.

Although we cannot conclude with certainty from the comparison between these data and the models that the evaporation is purely one dimensional, it does show that a model based on 1D evaporation describes the forced evaporation in our Ioffe trap at low temperatures much better than a model based on 3D evaporation.

C. Optimized 1D evaporation

Armed with the knowledge that evaporation in our Ioffe trap is more 1D than 3D, we aimed to arrive at the highest attainable phase-space density, using the model (described in detail below) based on 1D evaporation to optimize the trajectory through phase space. The optimal model trajectory was found by computer optimization of the evaporation process to obtain the highest phase-space density. In this optimization the currents through four of the five magnets were used as adjustable parameters, taking into account the starting conditions and the technical constraints imposed by the apparatus.

High radial confinement during loading of the trap maximizes the number of trapped atoms, and assures the highest initial densities for the evaporation experiment. On the other hand, tight radial confinement leads to very small samples at low temperatures, making the optical thermometry difficult. Therefore we reduce the α coefficient during the first stages of the ramp. The ramp-down rate of the radial confinement coils was limited by the risk of quenching of the superconducting wires. The final current configuration was fixed to be sure that a trap of finite depth remained at the end.

To simplify the calculation of the optimal ramp settings further, the ramp was divided into seven linear current sweeps. Both the duration of every linear sweep and the destination currents were optimized using a computer program based on the one-dimensional evaporation model, but including the full z dependence of the field. It was checked that in both the radial and axial directions $\epsilon_t/\hbar\omega$ decreased monotonically, with ω the radial or axial trap oscillation frequency. This indicates that no empty trap states are introduced, which is necessary for the model to be valid, as will be discussed in Sec. VI C.

The effect of adiabatic compression or decompression of the trap is also taken into account in the model. However, because the product of curvatures $\omega_\perp^2\omega_z$ in the optimized ramp turns out to be constant within 20%, this hardly influences the result. We also found that during the simulated evolution the effective-volume exponent γ remains in the narrow range $1.4<\gamma<1.6$. This means that adiabatic changes of the phase-space density [15] do not play an essential role in the present experiments.

It is interesting to look at the evolution of the truncation parameter η during the optimized ramp. This is depicted in Fig. 4. Note that the value of η is, apart from some oscillations, steadily decreasing. This reflects the need for accelerated evaporation due to the increasing importance of dipolar heating with decreasing temperature. The oscillations are a result of the linear sweeps which form the building blocks of the total ramp. This indicates that, in principle, a better optimized ramp would be possible by using another optimization scheme which can deal with more complicated (smoother) ramps, or simply a larger number of linear ones. However, the fact that the wiggles in η are hardly reflected in Fig. 3 indicates that this could not have gained more than a few percent in, e.g., the density, because evaporation at a certain η corresponds to a certain slope in the T-n_0 plane.

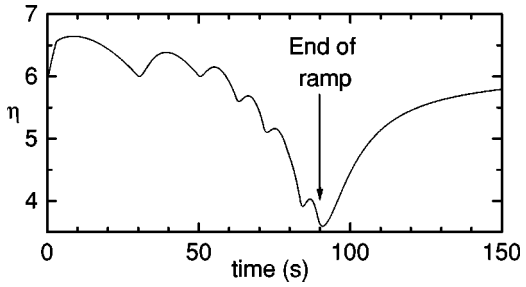

FIG. 4. Calculated evolution of the truncation parameter η in a ramp optimized using the model based on 1D evaporation.

We typically start with 4×10^{12} atoms loaded into the trap at a density of 7×10^{12} cm^{-3} and a temperature of 0.11 K. Because spectroscopy is difficult if the trapping field is changing, we repeated the ramp a number of times, the first time stopping after the second linear sweep, and the next time stopping after the third linear sweep until the total ramp of seven sweeps, in order to map out the complete trajectory. Every time that we broke off the ramp, the currents in the magnets were allowed to relax to the currents set by the power supplies at that moment. We also simulated these partial ramps, to compare with data. Before every (partial) ramp, we reloaded the cell with atomic hydrogen. The loading procedure leads to roughly the same starting conditions, but because the loading depends on the temperature of the cell, variations of order 30% in density can occur. Figure 5 shows the ramps to step 2,3,...,7. The curve labeled 7 is the complete optimized ramp.

There is reasonable agreement between the data and the 1D model for the ramps to step 5. The discrepancy between the model and the data at steps 6 and 7 are probably due to

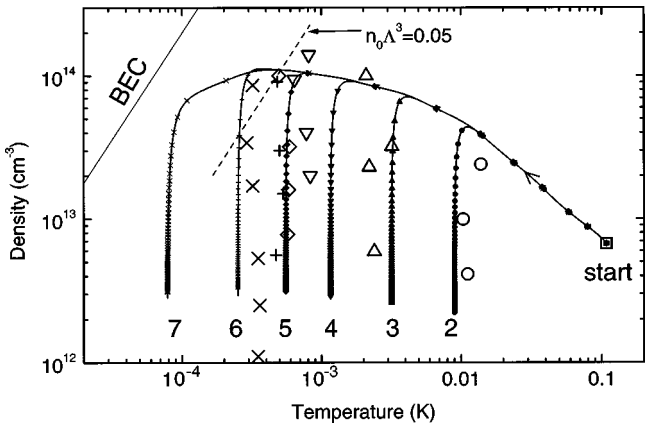

FIG. 5. Evolution of trapped gas on the n_0-T plane. The curves are simulations based on 1D evaporation. The solid symbols on the theoretical curves are spaced 10 s apart. The larger, open symbols are experimental data points. The solid circles are measured in a ramp to step 2. The corresponding theoretical curve has open circles, etc.

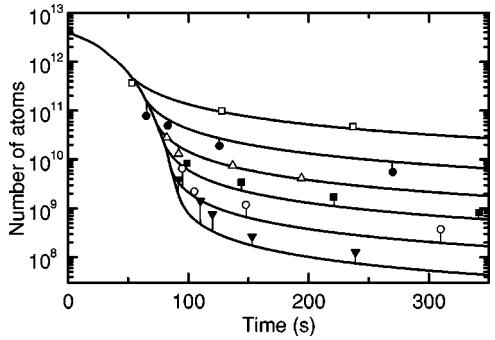

FIG. 6. Evolution of the number of atoms as a function of time for ramp steps 2 (top) to 7 (bottom). The curves are simulations based on 1D evaporation. The experimental data points are connected with the corresponding theoretical curve by a vertical line.

the fact that the spectroscopy becomes less sensitive to the temperature below 1 mK. Spectroscopy is better at determining the number of atoms and, as can be seen in Fig. 6, the discrepancy is smaller. Also, deviation of the trap depth due to the stray fields becomes more important at small trap depths, as well as errors in the estimation of the calculated currents due to, e.g., neglect of the mutual inductances of the coils, and noise of the power supplies. Other possible sources of systematic errors are heating of the cloud by the probe light and heating by background gas produced by the eddy-current heating of the cell when ramping the magnets.

The highest phase-space density achieved can be found in the upper left corner of Fig. 5: $n_0\Lambda^3 \simeq 0.05$, a little more than an order of magnitude short of BEC. This represents, we believe, the limit of the present apparatus. At the end of this paper we will discuss how this limit might be circumvented.

IV. MODELING THE TRAPPED GAS

A. Introduction

The first descriptions of evaporative cooling assumed that the trapped atoms had energies distributed according to a Boltzmann distribution truncated at the trap depth [22–25]. Luiten, Reynolds, and Walraven [11] proved by numerical solution of the Boltzmann equation that for nondegenerate Bose gases the evaporation process conserves the truncated Boltzmann distribution rather accurately. Expressions were derived for the evolution of the thermodynamic quantities and for the rate of evaporation. Walraven extended this description by incorporating the effect of continuously reducing the trap depth, introducing the notion of spilling [12]. Berg-Sørensen discussed how to incorporate the time dependence of the trap parameters for an IQ trap [26].

Detailed modeling of evaporative cooling is possible using the direct simulation Monte Carlo (DSMC) method [27,28]. This powerful method, originally introduced for calculations of gas dynamics [29], does not require any assumptions regarding the form of the distribution function. The DSMC method has been used to study the difference between 3D and 1D evaporation [27], including the effect of quantum statistics [28]. It is also well suited to study evaporative cooling in complicated situations, such as when the collision cross section is energy dependent or when the mean free path of the atoms is comparable to the size of the gas cloud. It demands, however, rather fast computers, especially if evaporation ramps are to be optimized.

Here we will work with the thermodynamic description, generalizing it to include evaporative cooling in two limiting cases (3D and 1D), and to include the time variation of both the depth of the trap and the shape of the confining potential. As explained in Sec. II A, we limit our modeling of the trapped gas to the description of an ideal gas in the Knudsen regime. In this section we will discuss aspects of the modeling that are independent of the nature (dimensionality) of the truncation. Later, we discuss the variables and equations that are specific to the 1D (Sec. V) or 3D case (Sec. VI).

To include the time evolution of the trap in the formalism in a simple way, we introduce a single symbol θ, which is an abbreviation for the set of independent control parameters needed to determine the trapping potential. In our case these are the five independently controllable currents through the different coil sets. In principle θ could include the frequency of a rf field applied for evaporation. In yet other versions of the model θ might represent a single parameter. For example, if only the truncation energy ϵ_t is varied then θ can be identified with ϵ_t. The trapping potential is, in general, a function of $\mathbf{r}$ which depends parametrically on θ. With the passage of time θ varies, as determined by the ramp program imposed upon the power supplies.

B. Thermodynamics

We describe the trapped gas by its classical phase-space distribution of atoms $f(\mathbf{r},\mathbf{p})$, which we normalize as in Ref. [11], such that the total number of atoms, N, is given by

$$N=(2\pi\hbar)^{-3}\int d^3r\, d^3p\, f(\mathbf{r},\mathbf{p}). \tag{4}$$

Note that, with this normalization, f corresponds to quantum-mechanical occupation numbers. Here we consider a nondegenerate gas, i.e., with $f \ll 1$. To allow a thermodynamic description we use a generalization of the truncated Boltzmann approximation employed in Ref. [11]. We assume that an atom can be identified as ''trapped'' or ''untrapped'' on the basis of its instantaneous position in phase space, that the untrapped atoms are efficiently removed, and that the trapped atoms are described by a thermal distribution. More precisely, the phase-space distribution is assumed to have the form of an equilibrium distribution

$$f(\mathbf{r},\mathbf{p})=n_0\Lambda^3 e^{-U(\mathbf{r})/kT}e^{-p^2/2mkT} \tag{5}$$

for $\mathbf{r},\mathbf{p}$, such that the atom is trapped and to be zero elsewhere. This distribution is characterized by two parameters: the (maximum) phase-space density $n_0\Lambda^3$ and the temperature T. The only difference between the distribution in the case of 1D and 3D evaporation is the criterion for truncation. In the case of 1D evaporation, an atom leaves the trap if its z energy $\epsilon_z = U_z(z)+p_z^2/2m$ exceeds ϵ_t and, hence, $f=0$ for $\epsilon_z > \epsilon_t$. In the case of 3D evaporation an atom escapes the trap if its total energy $\epsilon = U(\mathbf{r})+p^2/2m$ exceeds ϵ_t and, hence, $f=0$ for $\epsilon > \epsilon_t$.

Although a true thermal equilibrium does not exist in an evaporating gas, the truncated Boltzmann approximation for the phase-space distribution allows us to adopt many of the methods and results of statistical mechanics. A central quan-

tity is the effective volume $V_e(T,\theta)$, defined by $V_e = N/n_0$. The effective volume is Λ^3 times the single-particle partition function (see Ref. [11]), and hence can be used to calculate all thermodynamic functions. We limit ourselves to conditions with sufficient particles to be insensitive for the choice of ensemble. The energy E of the trapped gas is given by [30]

$$E = (\tfrac{3}{2} + \gamma) NkT, \tag{6}$$

where $\gamma = (T/V_e)(\partial V_e/\partial T)_\theta$, the partial derivative being evaluated at constant θ (i.e., holding the trap fixed). For a full thermal (not truncated) distribution an atom has an average kinetic energy $(3/2)kT$ and an average potential energy γkT. For a truncated distribution, this interpretation of the two terms in Eq. (6) is not legitimate, although their sum is still the total energy. The entropy S of the trapped gas is given by

$$S = Nk(\tfrac{5}{2} + \gamma - \ln n_0 \Lambda^3). \tag{7}$$

This expression can be derived from the partition function [15], even when the partition function refers to a truncated phase-space distribution. The entropy of a truncated gas is smaller than the entropy of a gas with the same N and E in thermal equilibrium in a deep trap [31].

The energy and entropy of the trapped gas are functions of N, T, and θ, which act as the sole independent thermodynamic variables of the trapped gas. In terms of these variables the time dependence of E and S can be written as

$$\dot{E} = \left(\frac{3}{2} + \gamma\right) kT\dot{N} + C\dot{T} + \left(\frac{\partial \gamma}{\partial \theta}\right)_T NkT\dot{\theta} \tag{8}$$

and

$$\frac{\dot{S}}{k} = \left(\frac{S}{kN} - 1\right)\dot{N} + C\frac{\dot{T}}{T} + \left\{\left(\frac{\partial \gamma}{\partial \theta}\right)_T + \frac{1}{V_e}\left(\frac{\partial V_e}{\partial \theta}\right)_T\right\} N\dot{\theta}, \tag{9}$$

with the heat capacity $C \equiv (\partial E/\partial T)_{N,\theta}$ given by the usual expression [11]

$$C = \left(\frac{3}{2} + \gamma + T\frac{\partial \gamma}{\partial T}\right) kN. \tag{10}$$

The last term in Eq. (8) is, in the special case that only the trap depth ϵ_t is varied and the potential is otherwise unchanged, the product of $\dot{\epsilon}_t$ and the ''heat of truncation'' [12,26].

C. Differential equations for the evolution of the gas

To determine the time evolution of the trapped gas, we numerically integrate the differential equations for N and T:

$$\dot{N} = \dot{N}_{\rm ev} + \dot{N}_\theta + \dot{N}_{\rm rel}, \tag{11a}$$

$$C\dot{T} = \dot{E}_{\rm ev} + \dot{E}_\theta + \dot{E}_{\rm rel} - \left(\frac{3}{2} + \gamma\right) kT\dot{N} - \left(\frac{\partial \gamma}{\partial \theta}\right)_T NkT\dot{\theta}. \tag{11b}$$

Equation (11a) simply reflects that $\dot{N}$ is the sum of the independent contributions $\dot{N}_{\rm ev}$, $\dot{N}_\theta$, and $\dot{N}_{\rm rel}$ for the rate of change of the number of trapped atoms due to evaporation, trap changes (spilling), and dipolar relaxation, respectively. In Eq. (11b) the rate of change of the energy of the trapped gas is also written as a sum of the independent contributions $\dot{E}_{\rm ev}$, $\dot{E}_\theta$, and $\dot{E}_{\rm rel}$ for the rate of change of energy due to evaporation, trap changes (spilling and work), and dipolar relaxation, respectively. At each time step $\dot{N}$ and $\dot{T}$ are calculated—all contributions and auxiliary quantities are either known functions of N, T, and θ or can be determined by numerical differentiation [32]. We will now consider the contribution of evaporation, trap changes, and dipolar relaxation in turn.

D. Evaporation

Elastic collisions between the trapped atoms lead to evaporation by promoting atoms to untrapped states. We assume isotropic (s-wave) scattering with a velocity-independent collision cross section $\sigma = 8\pi a^2$, where a is the scattering length. Evaporation causes a rate of change of atom number, $\dot{N}_{\rm ev}$, and energy, $\dot{E}_{\rm ev}$, which we can express in terms of effective volumes $V_{\rm ev}$ and $W_{\rm ev}$ introduced as follows [11]:

$$\dot{N}_{\rm ev} = -n_0^2 \sigma \bar{v} e^{-\eta} V_{\rm ev}, \tag{12a}$$

$$\dot{E}_{\rm ev} = \dot{N}_{\rm ev}\left(\eta + \frac{W_{\rm ev}}{V_{\rm ev}}\right) kT, \tag{12b}$$

with $\eta = \epsilon_t/kT$, and the thermal velocity defined as $\bar{v} = \sqrt{8kT/\pi m}$. This shows explicitly the dependence on the atomic collision cross section σ and the gas temperature T and reference density n_0. The effective volumes depend only on the trapping potential, the truncation parameter η, and the nature of the phase-space truncation (dimensionality of evaporation). For 1D truncation we derive these volumes in Sec. V. For 3D truncation this was done in Ref. [11]; for convenience we reproduced the expressions in Ref. [33].

E. Spilling and work

If the trapping potential is changed, some atoms are lost from the trap due to spilling, and the remaining atoms may change their energy (i.e., do work on the magnet power supplies). Spilling is distinct from evaporation—it occurs even in the absence of collisions. In the 1D situation where the transverse and longitudinal motions of the atoms are dynamically uncoupled, spilling can lead to anisotropic energy distributions with $T_z < T_\perp$ if the potential $U_z(z)$ is varied on a time scale short compared to the thermalization time of the trapped gas, but slowly compared with the oscillation period for z motion [17]. This was partially the case in the experiment distinguishing 1D from 3D evaporation, presented in Sec. III B. In our other experiments, however, we typically have variations of the trapping potential slow compared to the collision time scale, and in our model will assume that the gas distribution is described by a single temperature.

By changing the trapping potential or trap depth (via the control parameters θ) we induce a rate of change $\dot{N}_\theta$ in the number of trapped atoms and $\dot{E}_\theta$ in the total energy. These quantities depend upon the nature of the phase-space truncation (3D or 1D). In principle, they can be derived from the Boltzmann equation for a gas in a time-dependent potential, at least for the case of 3D truncation [26].

Atoms are spilled from the trap because they occupy quantum bound states which are lost from the trapping potential. The rate of change of the number of trapped atoms due to spilling, $\dot{N}_\theta$, is found straightforwardly by counting the atoms in the lost states. Expressions are derived for 1D truncation in Sec. V C, and for 3D truncation in Sec. VI C. For a fixed trap shape, $\dot{N}_\theta$ is simply related to the rate of change of the trap depth [12]. This is not true in general, because variation of the shape of the trapping potential can lower the energy of atoms near the trap edge (adiabatic expansion), and prevent them from being spilled even if their original energy exceeded the final trap depth.

To calculate the rate of change of the energy of the trapped gas due to changing the trap, $\dot{E}_\theta$, we must account for the energy of the spilled atoms and for the effect of trap variations on the energy of those atoms which remain trapped (i.e., the work done by the trapped gas against the confining potential). For a deep trap, changes in the trap shape can even lead to adiabatic variations of the peak phase-space density (degeneracy) of the gas [15]. The simplest way to derive $\dot{E}_\theta$ is through consideration of the entropy of the gas. As the trap is varied, entropy is carried away by the spilled atoms. Within the truncated Boltzmann approximation, changing the trap does not cause any other entropy changes because the phase-space distribution is always thermal. Hence the rate of change of the entropy of the trapped gas due to variation of the trapping potential, $\dot{S}$, is proportional to $\dot{N}_\theta$. We write

$$\dot{S}_\theta = \dot{N}_\theta s_\theta, \tag{13}$$

where the entropy removed per spilled atom, s_θ, depends on the nature of the truncation. We calculate s_θ for 1D truncation in Sec. V, and for 3D truncation in Sec. VI.

Once we know s_θ, the rate of change of the energy of the trapped gas follows from substituting $\dot{T}$ obtained from Eq. (9) into Eq. (8). This gives

$$\dot{E}_\theta = \dot{N}_\theta (s_\theta + k \ln n_0 \Lambda^3) T - \frac{NkT}{V_e} \left(\frac{\partial V_e}{\partial \theta} \right)_T \dot{\theta}. \tag{14}$$

This expression for $\dot{E}_\theta$ can then used in Eq. (11b) for the evolution of the temperature of the trapped gas.

An easy way to calculate s_θ is by considering the special case of pure spilling (reducing the truncation energy ϵ_t while preserving all other trap parameters). In this case T and n_0 are constant, allowing us easily to determine s_θ as a function of T, n_0, θ, and the type of truncation. For more complicated changes of the trapping potential s_θ will be the same. All that matters is that spilled atoms come from the truncation edge.

In an infinitely deep trap ($\dot{N}_\theta = 0$), the last term of Eq. (14) gives rise to adiabatic (de)compression of the thermal cloud, and the derivative of γ in Eq. (11b) gives rise to a variation of $n_0 \Lambda^3$ proportional to e^γ [15]. In a finite depth trap these effects cannot be separately attributed to these two derivatives. However, it can easily be verified for a finite-depth power-law trap that $n_0 \Lambda^3 \propto e^\gamma$ if no atoms are lost. Of course, for a real gas in a finite-depth trap the collisions required to maintain the truncated Boltzmann distribution will also lead to evaporative cooling, which will tend to obscure the adiabatic contribution to changes of the phase-space density.

F. Dipolar relaxation

Inelastic collisions between atoms are also important for the evolution of the trapped gas. For atomic hydrogen, spin relaxation in binary collisions is the dominant inelastic process. The contributions due to dipolar relaxation of the atoms in binary collisions, $\dot{N}_{\rm rel}$ and $\dot{E}_{\rm rel}$, are calculated assuming a temperature independent rate constant G depending upon magnetic field as calculated in the literature [34]. The loss rate follows from $\dot{N}_{\rm rel} = -n_0^2 G V_{2e}$, where $V_{2e} = \int d^3 r [n(\mathbf{r})/n_0]^2$ is the effective volume for binary collisions. For the determination of $\dot{E}_{\rm rel}$, given by $\dot{E}_{\rm rel} = (3/2 + \gamma_2) kT \dot{N}_{\rm rel}$, we use the two-atom energy parameter $\gamma_2 \equiv (T/2V_{2e}) \partial V_{2e}/\partial T$. Because the average energy that particles take away after an inelastic collision is much less than the trap depth and because collisions predominantly occur in the core of the distribution, the truncation is not important for the determination of γ_2.

V. 1D MODEL DETAILS

In this section we will discuss the features specific to the model with 1D evaporation, which we have used to analyze and optimize our experiments.

A. 1D thermodynamics

In the case of 1D evaporation, the phase-space distribution $f(\mathbf{r},\mathbf{p})$ is truncated on the basis of the z energy of the atom, given by $\epsilon_z \equiv U_z(z) + p_z^2/2m$. That is, it has the Boltzmann form Eq. (5) in the region of phase space where $\epsilon_z < \epsilon_t$, and is zero elsewhere. In this case the density distribution of atoms in position space, given by $n(\mathbf{r}) = (2\pi\hbar)^{-1} \int d^3 p f(\mathbf{r},\mathbf{p})$, is

$$n(\mathbf{r}) = n_0 e^{-U(\mathbf{r})/kT} \ \mathrm{erf} \ \sqrt{\frac{\epsilon_t - U_z(z)}{kT}}. \tag{15}$$

The error function $\mathrm{erf}(x) \equiv 2\pi^{-1/2} \int_0^x \exp(-t^2) dt$ may also be written as $P(\frac{1}{2}, x^2)$, where P is the incomplete γ function [35]. This density distribution is used in the calculation of the optical spectrum of the trapped gas in our experiments.

For a trap potential which is separable into transverse and longitudinal parts, the effective volume V_e can be written as the product of an effective area A_e (transverse), given by

$$A_e = \int_{-\infty}^{\infty} \int_{-\infty}^{\infty} dx \, dy \, e^{-U_\perp(x,y)/kT}, \tag{16}$$

and an effective length L_e (longitudinal), given by

$$L_e = \int_{z_1}^{z_2} dz\ e^{-U_z(z)/kT}\ \mathrm{erf}\ \sqrt{\frac{\epsilon_t - U_z(z)}{kT}}, \tag{17}$$

where z_1 and z_2 are the turning points—the two solutions for z of the equation $\epsilon_t = U_z(z)$. When the transverse confinement is harmonic, we have $A_e = 2\pi kT/m\omega_\perp^2$. For the case of a potential of the form of Eq. (3), the effective area is given by

$$A_e = 4\lambda_x\lambda_y\Gamma(\delta_x+1)\Gamma(\delta_y+1)(kT)^{\delta_x+\delta_y}, \tag{18}$$

and the effective length is given by

$$L_e = 2\lambda_z\Gamma(\delta_z+1)P(\delta_z+1/2,\eta)(kT)^{\delta_z}, \tag{19}$$

where λ_x, λ_y, and λ_z are the scaling parameters of Eq. (3). The average energy of a trapped atom, E/N, given by Eq. (6), is determined by T and γ. In the case of a separable potential we can write $\gamma = \gamma_\perp + \gamma_z$, with $\gamma_\perp = (T/A_e)(\partial A_e/\partial T)_\theta$ and $\gamma_z = (T/L_e)(\partial L_e/\partial T)_\theta$. For harmonic transverse confinement, $\gamma_\perp = 1$. For power-law potentials of the form given by Eq. (3), we have $\gamma_\perp = \delta_x + \delta_y$ and

$$\gamma_z = -\frac{1}{2} + a\frac{P_{a+1}}{P_a}, \tag{20}$$

with $a = \delta_z + 1/2$ and the abbreviation $P_a \equiv P(a,\eta)$ for the incomplete γ function evaluated at the dimensionless trap depth η [36]. The effective exponent γ_z always lies between $-\frac{1}{2}$ (for $\eta = 0$) and δ_z (for $\eta = \infty$). For general $U_z(z)$, we evaluate γ_z by numerical integration along the trap axis.

In our modeling we use expressions appropriate to a harmonic transverse potential $U_\perp$, and evaluate longitudinal quantities like L_e and γ_z by numerical integration. The derivative $(\partial\gamma/\partial T)_\theta$ needed for the specific heat is found by numerical differentiation of γ. For a general power-law potential [Eq. (3)], the heat capacity (at constant θ and N) is given by

$$C = Nk\left\{1 + \delta_x + \delta_y + a\,\frac{P_{a+1}}{P_a}\left[(a+1)\frac{P_{a+2}}{P_{a+1}} - a\frac{P_{a+1}}{P_a}\right]\right\}. \tag{21}$$

B. 1D evaporation rate

Evaporation contributes to particle and energy loss according to Eq. (12). Here we employ kinetic theory to calculate the effective volumes V_{ev} and W_{ev} for the case of 1D evaporation. The volume V_{ev} is found by considering all pair collisions which occur per unit time in a gas described by the z-truncated Boltzmann distribution, summing all atoms which are promoted to longitudinal energy $\epsilon_z > \epsilon_t$. The calculation of the ''excess energy'' volume W_{ev} is analogous, but the total energy of the escaping atoms is summed.

Consider a collision, at position $\mathbf{r}$, of an atom of momentum $\mathbf{p}_1$ with an atom of momentum $\mathbf{p}_2$. To simplify matters we introduce the average momentum $\overline{\mathbf{p}} = (\mathbf{p}_1 + \mathbf{p}_2)/2$ and the relative momentum $\mathbf{q} = (\mathbf{p}_1 - \mathbf{p}_2)/2$. Collisions conserve $\overline{\mathbf{p}}$ and reorient $\mathbf{q}$ (according to an isotropic distribution for s-wave scattering). The number of collisions in volume d^3r at $\mathbf{r}$ during time dt involving a pair of atoms with average momentum in volume $d^3\overline{p}$ at $\overline{\mathbf{p}}$ and relative momentum in volume d^3q at $\mathbf{q}$ is equal to $\Gamma(\mathbf{r},\overline{\mathbf{p}},\mathbf{q})d^3r\ d^3\overline{p}\ d^3q\ dt$, where

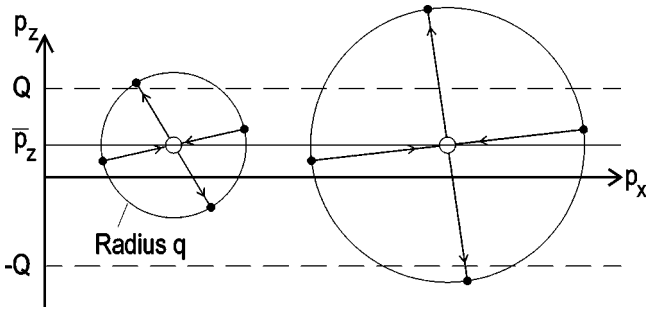

FIG. 7. Collision spheres for calculation of 1D evaporative cooling, projected onto the x-z plane. Atoms are trapped if their z momentum lies between $-Q$ and Q. The sphere radius is the relative momentum q. Left: $Q - \overline{p_z} < q < Q + \overline{p_z}$; only one atom can evaporate. Right: $q > Q + \overline{p_z}$; one or both atoms can evaporate.

$$\Gamma = \frac{8\sigma}{(2\pi\hbar)^6}\left|\frac{\mathbf{q}}{m}\right| f(\mathbf{r},\overline{\mathbf{p}}+\mathbf{q})f(\mathbf{r},\overline{\mathbf{p}}-\mathbf{q}), \tag{22}$$

with $\sigma = 8\pi a^2$, m the atomic mass, and the 8 arriving from the Jacobian $d^3p_1 d^3p_2 = 8d^3\overline{p}d^3q$. To sum all collisions we integrate over all of the six-dimensional $(\overline{\mathbf{p}},\mathbf{q})$ space.

Figure 7 shows the relevant collision geometry in momentum space. For a given axial coordinate in the trap, z, an atom will escape if it acquires a z momentum whose magnitude exceeds the local escape momentum $Q(z)$ given by $Q^2/2m = \epsilon_t - U_z(z)$. The relevant quantities are $\overline{p_z}$ (the z component of the average momentum, conserved in collision), q (the magnitude of the relative momentum, also conserved), q_z (the z component of the relative momentum before collision), and q_z' (the z component of the relative momentum after collision). By symmetry we need only consider $\overline{p_z}, q_z > 0$. Because the distribution of relative momentum after collision is isotropic, q_z' is distributed uniformly between 0 and q. Because we are interested in the fraction of the atoms that escape per collision, we may choose $q_z' > 0$. Depending on the momenta involved, one or two atoms can escape in a collision (in contrast to 3D evaporation, where only one atom can be lost per collision). The left sphere in Fig. 7, where $Q - \overline{p_z} < q < Q + \overline{p_z}$ depicts the first situation where only one atom can be lost from the trap. The second situation is depicted by the right sphere in Fig. 7, where $q > Q + \overline{p_z}$ and two atoms can be lost.

The rate at which atoms are lost from the trap is the integral, over position, average momentum and relative momentum, of the product of the collision kernel Γ given by Eq. (22), and the mean number of atoms leaving the trap per collision. For the left sphere in Fig. 7 $[q < Q(z) + \overline{p_z}]$ the mean number is just

$$\frac{1}{q}\int_{Q(z)-\overline{p_z}}^{q} dq_z'. \tag{23}$$

For the right sphere in Fig. 7 $[q > Q(z) + \overline{p_z}]$, two contributions should be added: the first corresponding with the situ-

ation that only one atom escapes (though there is enough total energy for the escape of two), and the second in which two atoms escape, yielding the mean number

$$\frac{1}{q}\left[\int_{Q(z)-\bar{p}_z}^{Q(z)+\bar{p}_z} 1\, dq_z' + \int_{Q(z)+\bar{p}_z}^{q} 2\, dq_z'\right]. \tag{24}$$

In addition, we note that the $\int d^3q$ integration over relative momenta before the collision (with $q_z>0$) can be written as

$$\int d^3q = 2\pi \int_0^{Q(z)-\bar{p}_z} dq_z \int_{Q(z)-\bar{p}_z}^{\infty} q\, dq, \tag{25}$$

where the dq_z integration is limited to select those collisions which occur in a truncated distribution. The dq integration should be split further into two parts corresponding to the two situations of Fig. 7.

From the above considerations we find the following explicit expression (exact within the 1D truncated Boltzmann approximation) for the rate of change of number of trapped atoms, $\dot{N}_{\rm ev}$, and their energy, $\dot{E}_{\rm ev}$:

$$\begin{aligned}\begin{pmatrix}\dot{N}_{\rm ev}\\ \dot{E}_{\rm ev}\end{pmatrix} = \frac{-64\pi\sigma n_0^2\Lambda^6}{(2\pi\hbar)^6 m}\int_{-\infty}^{\infty}\int_{-\infty}^{\infty} dx\, dy e^{-2U_\perp/kT}\int_{z_1}^{z_2} dz\, e^{-2U_z/kT}\int_{-\infty}^{\infty}\int_{-\infty}^{\infty} d\bar{p}_x d\bar{p}_y e^{-(\bar{p}_x^2+\bar{p}_y^2)/mkT}\int_0^{Q} d\bar{p}_z e^{-\bar{p}_z^2/mkT}\int_0^{Q-\bar{p}_z} dq_z \\ \times\left\{\int_{Q-\bar{p}_z}^{Q+\bar{p}_z} dq\; q e^{-q^2/mkT}\int_{Q-\bar{p}_z}^{q} dq_z'\begin{pmatrix}1\\ \epsilon_+\end{pmatrix} + \int_{Q+\bar{p}_z}^{\infty} dq\; q e^{-q^2/mkT}\left[\int_{Q-\bar{p}_z}^{Q+\bar{p}_z} dq_z'\begin{pmatrix}1\\ \epsilon_+\end{pmatrix} + \int_{Q+\bar{p}_z}^{q} dq_z'\begin{pmatrix}2\\ \epsilon_+ + \epsilon_-\end{pmatrix}\right]\right\},\end{aligned} \tag{26}$$

where z_1 and z_2 are the two solutions for z of the equation $\epsilon_t = U_z(z)$. The energy of the atom on the upper $(+)$ or lower $(-)$ hemisphere in Fig. 7 after the collision is $\epsilon_\pm \equiv U_\perp + U_z + (\bar{\mathbf{p}} \pm \mathbf{q}')^2/2m = U_\perp + U_z + (\bar{p}^2 + q^2 + 2\bar{p}_x q_x' + 2\bar{p}_y q_y' \pm 2\bar{p}_z q_z')/2m$. The $\bar{p}_x q_x'$ and $\bar{p}_y q_y'$ terms will integrate to zero. The prefactor in Eq. (26) comprises the factors appearing in Eqs. (5) and (22), a factor of 4 due to the restriction to positive q_z and $\bar{p}_z$, and a factor 2π from the integral of azimuthal directions of $\mathbf{q}$ before collision.

In the calculation of $\dot{N}_{\rm ev}$, the integration over transverse average momentum may be done immediately: $\int_{-\infty}^{\infty}\int_{-\infty}^{\infty} d\bar{p}_x d\bar{p}_y \exp[-(\bar{p}_x^2+\bar{p}_y^2)/mkT] = \pi mkT$. The integration over the transverse position contributes to the prefactor of the remaining integrals the two-body effective area

$$A_{2e} = \int_{-\infty}^{\infty}\int_{-\infty}^{\infty} dx\, dy\, e^{-2U_\perp/kT}. \tag{27}$$

After some manipulations, the $\dot{N}_{\rm ev}$ part of Eq. (26) leads, with Eq. (12a), to the effective volume for the 1D evaporation from an arbitrary separable potential

$$V_{\rm ev} = A_{2e}\int_{z_1}^{z_2} dz\, e^{\kappa-\eta} F(\sqrt{2\kappa}), \tag{28}$$

where the local trap depth parameter is given by $\kappa(z) \equiv [\epsilon_t - U_z(z)]/kT$, and the function F is defined by

$$F(a) = \int_0^a dx\, e^{a^2/2-x^2}(a-x)\,\frac{\mathrm{erfc}(a-x)+\mathrm{erfc}(a+x)}{\sqrt{2}}, \tag{29}$$

with $\mathrm{erfc}(x) = 1-\mathrm{erf}(x)$. The argument a is the local escape momentum Q in units of the one-dimensional rms thermal momentum $\sqrt{mkT}$. The calculation of $\dot{E}_{\rm ev}$ proceeds similarly to that of $\dot{N}_{\rm ev}$. In fact we need $V_{\rm ev}$, because the volume $W_{\rm ev}$ depends on it, as can be seen from Eq. (12b). The integral over the transverse coordinates of the transverse energy is found to be $-n_0^2\sigma\bar{v}e^{-\eta}(5/4+\gamma_{2\perp})V_{\rm ev}kT$, with $\gamma_{2\perp} = (T/2A_{2e})\partial A_{2e}/\partial T$. The energy $(5/4+\gamma_{2\perp})kT$ is the average transverse energy of the atoms weighed with their collision rate. Since the transverse distribution is not truncated, we may use $A_{2e}(T) = A_e(T/2)$ and $\gamma_{2\perp}(T) = \gamma_\perp(T/2)/2$. With a harmonic potential for the x-y motion, $A_{2e}(T) = \pi kT/m\omega_\perp^2$ and $\gamma_{2\perp} = 1/2$. After the evaluation of the axial part, we obtain

$$W_{\rm ev} = (\tfrac{5}{4}+\gamma_{2\perp})V_{\rm ev} + A_{2e}\int_{z_1}^{z_2} dz\, e^{\kappa-\eta} G(\sqrt{2\kappa}), \tag{30}$$

where the function G is given by

$$\begin{aligned}G(a) = \int_0^a dx\, e^{a^2/2-x^2}(a-x) \\ \times\left[\frac{e^{-(a-x)^2}(a+x)+e^{-(a+x)^2}(a-x)}{2\sqrt{2\pi}}\right. \\ \left.+\left(\frac{x^2-a^2}{2}\right)\frac{\mathrm{erfc}(a-x)+\mathrm{erfc}(a+x)}{\sqrt{2}}\right].\end{aligned} \tag{31}$$

Equations (28) and (30) are consistent with the approximate expressions given for a particular trap shape in Ref. [10]. The functions F and G are plotted in Fig. 8. For efficient calculations, approximations of F and G are given in Ref. [37].

C. 1D spilling and work

The number of atoms in a trap can be written as the integral of the product of the density of states $\rho(\epsilon)$ and the energy distribution function $f(\epsilon)$ as $N = \int \rho(\epsilon) f(\epsilon) d\epsilon$, where $\rho(\epsilon) = (2\pi\hbar)^{-3}\int d^3p\; d^3r\, \delta(U + p^2/2m - \epsilon)$, and $f(\epsilon) = n_0\Lambda^3 \exp(-\epsilon/kT)$ for the nondegenerate regime (see, e.g., Ref. [12]). As is easily verified with the δ-function rule

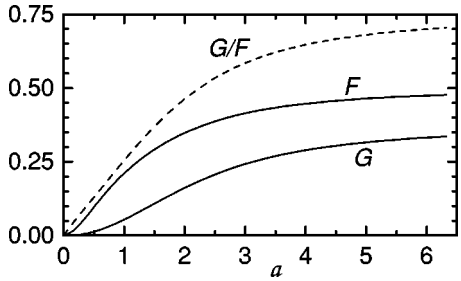

FIG. 8. Functions F and G used in calculation of 1D evaporation rate from an arbitrary trap. In the limit $a\to\infty$, $F\to\frac{1}{2}$ and $G\to\frac{3}{8}$. Also shown is the ratio G/F, which lies between 0 and 3/4.

$\int \delta(x-y)\,\delta(y-a)f(x)dy = f(x)\,\delta(x-a)$, this integral factors in a perpendicular and a longitudinal part, for a separable potential:

$$N=\int_0^\infty d\epsilon_\perp \rho_\perp(\epsilon_\perp)\int_0^{\epsilon_t} d\epsilon_z \rho_z(\epsilon_z) f(\epsilon_\perp+\epsilon_z), \tag{32}$$

with

$$\rho_\perp(\epsilon_\perp)=\frac{1}{(2\pi\hbar)^2}\int\int d^2p_\perp d^2r_\perp \delta\left(U_\perp+\frac{p_\perp^2}{2m}-\epsilon_\perp\right), \tag{33}$$

$$\rho_z(\epsilon_z)=\frac{1}{2\pi\hbar}\int\int dp_z dz\,\delta\left(U_z+\frac{p_z^2}{2m}-\epsilon_z\right). \tag{34}$$

Equation (32) is written for a trap of finite depth in the z direction only. The transverse integral in Eq. (32) can be expressed in terms of the effective area A_e, giving

$$N=\int_0^{\epsilon_t} d\epsilon_z \rho_z(\epsilon_z) A_e n_0 \Lambda e^{-\epsilon_z/kT}. \tag{35}$$

We see that the number of atoms in states with z energy ϵ_z is $A_e n_0 \Lambda e^{-\epsilon_z/kT}$. The number of states of one-dimensional motion bound in the potential $U_z(z)$, which we denote $\mathcal{N}_z$, is given by

$$\mathcal{N}_z=\int_0^{\epsilon_t} d\epsilon_z \rho_z(\epsilon_z)=\frac{2\sqrt{2m}}{2\pi\hbar}\int_{z_1}^{z_2}\sqrt{\epsilon_t-U_z(z)}\,dz. \tag{36}$$

For example, if $U_z(z)$ is harmonic, we have $\mathcal{N}_z=\epsilon_t/\hbar\omega_z$. The number of quantum states in the trap is a function only of the trap shape, parametrized by the set of independent coordinates θ.

To find the rate at which atoms are spilled from the trap as the potential is varied, we count the atoms in the quantum states of z motion which are lost from the trap, finding

$$\dot N_\theta = A_e n_0 \Lambda e^{-\eta}\dot{\mathcal{N}}_z, \tag{37}$$

i.e., $\dot N_\theta$ is the product of the number of atoms associated with each state of z motion at the trap edge and the rate of change of the number of these states [38]. We require that $\dot{\mathcal{N}}_z<0$, otherwise empty states are introduced at the trap edge and the picture of a truncated Boltzmann distribution would be destroyed. Hence the model can only describe situations in which the trap becomes shallower in the sense of supporting fewer bound states. This criterion is easily met when dealing with forced evaporation.

The rate of change of energy due to trap changes, $\dot E_\theta$, is calculated using the entropy argument discussed in Sec. IV. The entropy carried away by spilled atoms is found by considering the case of pure spilling (the trap edge is lowered while the potential shape is held constant). In this case, the rate of change of energy is given by

$$\dot E_\theta=(1+\gamma_\perp+\eta)kT\dot N_\theta, \tag{38}$$

because a particle barely escaping over the z barrier will on average take away kT of transverse kinetic energy, $\gamma_\perp kT$ of transverse potential energy, and exactly ϵ_t of z energy. Equation (38) is easily verified for a general power-law potential or an IQ potential, by taking the derivative of $(3/2+\gamma)NkT$ with respect to ϵ_t. Equations (6) and (7) allow us to write the entropy as $S=E/T+Nk(1-\ln n_0\Lambda^3)$. Differentiating this expression with respect to time, bearing in mind that for pure spilling both T and $n_0\Lambda^3$ are constant, we immediately find that the entropy removed by an atom spilled from a 1D truncated distribution is

$$s_\theta = k(2+\gamma_\perp+\eta-\ln n_0\Lambda^3). \tag{39}$$

Because s_θ is independent of the manner of trap change that caused the spilling, we can use it for changes of the trap other than pure spilling. Equation (14) gives the following expression for the rate of change of the energy of the trapped gas due to more general changes of the trapping potential:

$$\dot E_\theta=(2+\gamma_\perp+\eta)kT\dot N_\theta-\frac{NkT}{V_e}\left(\frac{\partial V_e}{\partial\theta}\right)_T\dot\theta. \tag{40}$$

Equations (37) and (40) are used in Eq. (11) for the evolution of N and T for the evaporating gas in the 1D model.

VI. 3D MODEL DETAILS

In this section we consider 3D (ergodic) evaporation. As in the 1D case, we choose the Ioffe quadrupole (IQ) trap as an example to evaluate quantities analytically.

A. 3D thermodynamics

The phase-space distribution function $f(\mathbf{r},\mathbf{p})$ given by the Boltzmann form [Eq. (5)] is now to be truncated on the basis of the total energy of the atom, as in Ref. [11]. This leads to a real-space density distribution

$$n(\mathbf{r})=n_0 e^{-U(\mathbf{r})/kT}P\left(\frac{3}{2},\frac{\epsilon_t-U(\mathbf{r})}{kT}\right). \tag{41}$$

The reference density n_0 is related to the number of atoms N by $n_0=N/V_e$, where the effective volume V_e for a IQ trap is given by

$$V_e=6A_{\rm IQ}\Lambda^3(kT)^4(P_4+\tfrac{2}{3}\xi\eta P_3), \tag{42}$$

with $P_a \equiv P(a,\eta)$ [36]. Furthermore, $\xi \equiv U_0/\epsilon_t$, and the trap constant $A_{\mathrm{IQ}} = (2m\pi^2)^{3/2}/[2(2\pi\hbar)^3\alpha^2\sqrt{\beta}]$.

The parameter γ is obtained from Eq. (6), and the known expression for the total energy of an energy-truncated gas in an IQ trap [11], giving

$$\gamma = -\frac{3}{2} + \frac{12P_5 + 6P_4\xi\eta}{3P_4 + 2P_3\xi\eta}. \tag{43}$$

The heat capacity C (at constant trap depth and number of atoms) is calculated straightforwardly by differentiating the total energy. We find that

$$C = 12Nk\,\frac{15P_4P_6 - 12P_5^2 + (10P_3P_6 - 6P_4P_5)\xi\eta + (4P_3P_5 - 3P_4^2)\xi^2\eta^2}{(3P_4 + 2\xi\eta P_3)^2}. \tag{44}$$

B. 3D evaporation rate

The rate of change of the number of atoms and the energy in the trapped gas, $\dot{N}_{\mathrm{ev}}$ and $\dot{E}_{\mathrm{ev}}$, are given by Eq. (12), with effective volumes for evaporation V_{ev} and W_{ev} calculated for three-dimensional truncation. For an IQ trap, expressions for these volumes were first derived in Refs. [11,33]. Integral expressions for the volumes V_{ev} and W_{ev} for 3D evaporation from an arbitrary trap, analogous to Eqs. (28) and (30), can be found in Ref. [11].

C. 3D spilling and work

To obtain $\dot{N}_\theta$ in the case of three-dimensional truncation, we calculate the number of quantum states in the trap, $\mathcal{N}$, by integrating the density of states $\rho(\epsilon)$ from 0 to ϵ_t. For an IQ trap, for which $\rho(\epsilon) = A_{IQ}(\epsilon^3 + 2U_0\epsilon^2)$, this leads to

$$\mathcal{N} = A_{\mathrm{IQ}}\left(\tfrac{1}{4}\epsilon_t^4 + \tfrac{2}{3}U_0\epsilon_t^3\right). \tag{45}$$

The rate of change of the number of trapped atoms due to spilling is then given by

$$\dot{N}_\theta = n_0\Lambda^3 e^{-\eta}\dot{\mathcal{N}}, \tag{46}$$

i.e., the product of the occupation number of states at the trap edge and the rate of change of the number of these states.

In the case of 3D truncation, to prevent the introduction of empty trap states it is not sufficient to assume that $\mathcal{N}$ decreases in time. Anisotropic variations of the trap can lead to introduction of empty states, spoiling the picture of a truncated Boltzmann distribution, even while decreasing the total number of states. However, during forced evaporation the trap depth is typically so strongly reduced that no significant introduction of empty states occurs due to variation of the shape of the trapping potential. In other words, states are lost from the trap in all directions. For a harmonic trap this concept can be made precise: empty states are not introduced if $\epsilon_t/\hbar\omega_x$, $\epsilon_t/\hbar\omega_y$, and $\epsilon_t/\hbar\omega_z$ are all decreasing functions of time.

The rate of change of energy of the trapped gas due to trap changes, accounting both for the spilling of atoms and for the work done by the trapped atoms as the trap is deformed, is determined, as in the 1D case, using the entropy argument introduced in Sec. IV. To find the entropy carried away by the spilled atoms, we consider ''pure spilling,'' where the truncation edge ϵ_t is reduced but the shape of the trap remains the same. In this case $\dot{E}_\theta = \epsilon_t\dot{N}_\theta$, and, because temperature T and (reference) density n_0 do not change, it is easily found that the entropy removed by each atom spilled over the trap edge is given by

$$s_\theta = k(1 + \eta - \ln n_0\Lambda^3). \tag{47}$$

Equation (14) can now be used to write the rate of change of energy due to more general trap changes as

$$\dot{E}_\theta = (1+\eta)kT\dot{N}_\theta - \frac{NkT}{V_e}\left(\frac{\partial V_e}{\partial\theta}\right)_T\dot{\theta}. \tag{48}$$

Equations (46) and (48) are used in Eq. (11) for the evolution of N and T for the evaporating gas in the 3D model.

VII. CONCLUSION

Our data show clearly that in an important class of trap geometries evaporation is bottlenecked by the nonergodic motion of the trapped atoms when the selection of escaping atoms is based on the energy in one direction only (1D evaporation), as predicted in Ref. [10]. This is in contrast to the situation at high temperatures, which was found to be described by a 3D evaporation picture [6].

We have derived an evaporation model based on the truncated Boltzmann approximation, which can describe either 3D or 1D evaporation. For 1D evaporation we present a kinetic theory derivation of the evaporation rate. The model improves on previously published models by describing processes such as atom spilling, adiabatic compression, and even adiabatic changes of the phase-space density. The expressions are well suited to optimize ramp trajectories for forced evaporation. For common traps analytic expressions are given for important quantities.

With this work, the low dimension of evaporation was identified as the bottleneck thus far preventing us from achieving Bose-Einstein condensation in trapped atomic hydrogen. Using a ramp optimized for 1D truncation, we reached a phase-space density $n_0\Lambda^3 \approx 0.05$ in our experiments. Our model predicts that BEC is attainable in hydrogen provided one can arrange sustained 3D evaporation.

A way to avoid the 1D evaporation bottleneck is to use magnetic-resonance-induced evaporation [7]. This would also allow evaporative cooling of the trapped gas without varying the currents in the superconducting magnets. For atomic hydrogen, it appears feasible to use the $F = m_F = 1$ to $F = m_F = 0$ hyperfine transition, for example, to eject atoms from the trap. For low B_0, the rf transition frequency is the

1.4-GHz hyperfine splitting. To obtain efficient evaporation, the rf need only pump energetic atoms to the untrapped hyperfine state on a time scale shorter than the mean time between collisions. Considerations such as those presented in Ref. [5] imply that a loop-gap resonator with a Q of 10^3 and a rf-field volume on the order of 1 cm^3 would yield efficient evaporation with a power dissipation of 1 μW, compatible with the cryo-environment. Another way to arrange 3D evaporation is to bring the high-energy wings of the gas in contact with a material pumping surface.

ACKNOWLEDGMENTS

We thank G. V. Shlyapnikov for interesting discussions. This work was part of a research program of the Stichting voor Fundamenteel Onderzoek der Materie (FOM), which is a subsidiary of the Nederlandse Organisatie voor Wetenschappelijk Onderzoek (NWO). M.W. acknowledges a TMR grant from the European Commission. The research of M.W.R. was supported by the Royal Dutch Academy of Arts and Sciences (KNAW).

[1] H. F. Hess, Phys. Rev. B **34**, 3476 (1986); C. Lovelace, C. Mehanian, T. J. Tommila, and D. M. Lee, Nature (London) **318**, 30 (1985).

[2] H. F. Hess, G. P. Kochanski, J. M. Doyle, N. Masuhara, D. Kleppner, and T. J. Greytak, Phys. Rev. Lett. **59**, 672 (1987).

[3] N. Masuhara, J. M. Doyle, J. C. Sandberg, D. Kleppner, and T. J. Greytak, Phys. Rev. Lett. **61**, 935 (1988).

[4] M. H. Anderson, J. R. Ensher, M. R. Matthews, C. E. Weiman, and E. A. Cornell, Science **269**, 198 (1995).

[5] W. Ketterle and N. J. van Druten, in *Advances in Atomic, Molecular and Optical Physics*, edited by B. Bederson and H. Walther (Academic, San Diego, 1996), Vol. 37, pp. 181–236, and references therein.

[6] O. J. Luiten, H. G. C. Werij, I. D. Setija, M. W. Reynolds, T. W. Hijmans, and J. T. M. Walraven, Phys. Rev. Lett. **70**, 544 (1993).

[7] D. E. Pritchard, K. Helmerson, and A. G. Martin, in *Atomic Physics 11*, edited by S. Haroche, J. C. Gay, and G. Grynberg (World Scientific, Singapore, 1989), p. 179; T. W. Hijmans, O. J. Luiten, I. D. Setija, and J. T. M. Walraven, J. Opt. Soc. Am. B **6**, 2235 (1989).

[8] I. D. Setija, H. G. C. Werij, O. J. Luiten, M. W. Reynolds, T. W. Hijmans, and J. T. M. Walraven, Phys. Rev. Lett. **70**, 2257 (1993).

[9] Making a potential-energy surface an absorber does not guarantee ergodic evaporation, since the atoms should reach the surface. A certain complexity of motion is also required. In a Ioffe trap this complexity is provided by the absence of complete axial symmetry.

[10] E. L. Surkov, J. T. M. Walraven, and G. V. Shlyapnikov, Phys. Rev. A **53**, 3403 (1996).

[11] O. J. Luiten, M. W. Reynolds, and J. T. M. Walraven, Phys. Rev. A **53**, 381 (1996).

[12] J. T. M. Walraven, in *Proceedings of the SUSSP 44 Conference on Quantum Dynamics of Simple Systems*, edited by G.-L. Oppo, S. M. Barnett, E. Riis, and M. Wilkinson (Institute of Physics, Bristol, 1996), pp. 315–352.

[13] A. Lagendijk, I. F. Silvera, and B. J. Verhaar, Phys. Rev. B **33**, 626 (1986); H. T. C. Stoof, J. M. V. A. Koelman, and B. J. Verhaar, *ibid.* **38**, 4688 (1988).

[14] J. M. Doyle, J. C. Sandberg, N. Masuhara, I. A. Yu, D. Kleppner, and T. J. Greytak, J. Opt. Soc. Am. B **6**, 2244 (1989).

[15] P. W. H. Pinkse, A. Mosk, M. Weidemüller, M. W. Reynolds, T. W. Hijmans, and J. T. M. Walraven, Phys. Rev. Lett. **78**, 990 (1997).

[16] T. Bergeman, G. Erez, and H. J. Metcalf, Phys. Rev. A **35**, 1535 (1987).

[17] E. L. Surkov, J. T. M. Walraven, and G. V. Shlyapnikov, Phys. Rev. A **49**, 4778 (1994).

[18] V. Bagnato, D. E. Pritchard, and D. Kleppner, Phys. Rev. A **35**, 4354 (1987).

[19] O. J. Luiten, H. G. C. Werij, I. D. Setija, M. W. Reynolds, T. W. Hijmans, and J. T. M. Walraven, in *Proceedings of the 13th International Conference on Atomic Physics*, edited by H. Walther, T. W. Hänsch, and B. Neizert (AIP, New York, 1993), p. 167.

[20] The L/R relaxation time is 1.2 s for the coil which determines the trap depth.

[21] O. J. Luiten, H. G. C. Werij, M. W. Reynolds, I. D. Setija, T. W. Hijmans, and J. T. M. Walraven, Appl. Phys. B: Photophys. Laser Chem. **59**, 311 (1994).

[22] J. M. Doyle, Ph.D. thesis, Massachusetts Institute of Technology, 1991 (unpublished).

[23] J. M. Doyle, J. C. Sandberg, I. A. Yu, C. L. Cesar, D. Kleppner, and T. J. Greytak, Physica B **194**, 13 (1994).

[24] K. B. Davis, M.-O. Mewes, and W. Ketterle, Appl. Phys. B: Photophys. Laser Chem. **60**, 155 (1995).

[25] O. J. Luiten, Ph.D. thesis, University of Amsterdam, 1993 (unpublished).

[26] K. Berg-Sørensen, Phys. Rev. A **55**, 1281 (1997); This Ref. states that several equations in Ref. [11] are in error. However, as explained in an erratum [*ibid.* **56**, 3308(E) (1997)], the two papers merely use different definitions of ξ.

[27] H. Wu and C. J. Foot, J. Phys. B **29**, L321 (1996).

[28] H. Wu, E. Arimondo, and C. J. Foot, Phys. Rev. A **56**, 560 (1997).

[29] G. A. Bird, *Molecular Dynamics and the Direct Simulation of Gas Flows* (Clarendon, Oxford, 1994).

[30] *Nota bene*: E/N, the average energy of a trapped atom, is not the chemical potential as unfortunately implied in Ref. [11]. The chemical potential is, as usual, given by $\mu = kT \ln(n_0\Lambda^3)$ for a gas far from degeneration.

[31] Davis, Mewes, and Ketterle [24] modeled ergodic evaporative cooling by a series of steps in which the high-energy tail of the energy distribution is cut off instantaneously, after which the gas rethermalizes to a full distribution. In our terminology this is a phase-space-density conserving truncation of the high-energy tail which removes energy and entropy, followed by a rethermalization in which phase-space density is gained even though entropy increases. If we begin with a truncated distribution, instantly set $\epsilon_t \to \infty$, and allow the gas to thermalize,

the entropy will of course increase. For a power-law trap, the change of entropy ΔS is given by $\Delta S/Nk = a[1 - P_{a+1}/P_a + \ln(P_{a+1}/P_a)] - \ln P_a$, with $a = 3/2 + \delta$ and $P_a \equiv P(a, \eta)$. This entropy change on thermalization is a monotonically decreasing positive function of η.

[32] In the computer simulation employing numerically determined magnetic fields, it is convenient to calculate the partial derivatives of temperature-dependent quantities such as γ with respect to θ using, e.g., $(\partial\gamma/\partial\theta)_T\dot{\theta} = (\gamma' - \gamma)/\Delta t$, where γ' is calculated ''in between'' time steps, using the trap of time $t + \Delta t$ but the temperature of time t.

[33] $V_{\rm ev} = \Lambda^3\zeta_\infty^0\{\eta - 5 + \xi\eta(2\eta/3 - 8/3) + e^{-\eta}[\eta^4/24 + \eta^3/3 + 3\eta^2/2 + 4\eta + 5 + \xi\eta(\eta^3/9 + 2\eta^2/3 + 2\eta + 8/3)]\}$, $W_{\rm ev} = \Lambda^3\zeta_\infty^0\{\eta - 6 + \xi\eta(2\eta/3 - 10/3) + e^{-\eta}[\eta^5/120 + \eta^4/12 + \eta^3/2 + 2\eta^2 + 5\eta + 6 + \xi\eta(\eta^4/36 + 2\eta^3/9 + \eta^2 + 8\eta/3 + 10/3)]\}$, with $\zeta_\infty^0 \equiv 6A_{\rm IQ}(kT)^4$.

[34] H. T. C. Stoof, J. M. V. A. Koelman, and B. J. Verhaar, Phys. Rev. B **38**, 4688 (1988). Simplified expressions can be found in R. van Roijen, Ph.D. thesis, University of Amsterdam, 1989 (unpublished).

[35] *Handbook of Mathematical Functions*, edited by M. Abramowitz and I. A. Stegun (Dover, New York, 1972).

[36] For integer a, $P_a = 1 - e^{-\eta}\Sigma_{m=0}^{a-1}\eta^m/m!$.

[37] The functions $F(a)$ and $G(a)$ can be approximated by $F(a) \approx 1/(1.946 + 2.82a^{-1.617})$ and $G(a) \approx 1/(2.707 + 16.20a^{-2.211})$. The relative deviations of these approximations are less than 1% in the region $1 < a < 6$ (i.e., for $\frac{1}{2} < \eta < 18$).

[38] A classical description of spilling is also possible. Consider the action $\oint p_z dz$ associated with the z motion of an atom (the integral is over one cycle of z motion). The maximum action for a given trap is the action for an atom of z energy equal to ϵ_t. Slowly lowering the depth of the trap, the action of each atom is constant, and the rate of spilling is just the rate at which atoms are left behind by the decreasing maximum action.